

Let's keep brainstorming title ideas. I don't think our results support the idea of 'episodes of rapid expansion'

Trevor Drees<sup>\*a,b</sup>, Brad M. Ochocki<sup>b</sup>, Scott L. Collins<sup>c</sup>, and Tom E.X. Miller<sup>b</sup>

<sup>a</sup>Department of Biology, Penn State University, State College, PA USA

<sup>b</sup>Program in Ecology and Evolutionary Biology, Department of BioSciences, Rice University, Houston, TX USA

<sup>c</sup>Department of Biology, University of New Mexico, Albuquerque, NM USA

April 19, 2021

---

<sup>\*</sup>thd5066@psu.edu

# 1 Abstract

2 **Encroachment**<sup>1</sup> of shrubs into adjacent grasslands has become an increasingly reported  
3 phenomenon across the world, and such encroachment is either pulled forward by high  
4 population growth at the low-density encroachment front or pushed forward by higher-  
5 density areas behind the front. However, at sites such as Sevilleta National Wildlife  
6 Refuge in central New Mexico, little is known about whether encroachment is pushed or  
7 pulled, and the dynamics of encroachment are not well-understood. Here, long-term en-  
8 croachment of creosotebush (*Larrea tridentata*), a native perennial shrub, stands in stark  
9 contrast with the stagnation in encroachment observed in recent decades. In order to  
10 better understand creosotebush encroachment at this site, we quantify it using a spatially  
11 structured population model where a wave of individuals travels at a speed governed by  
12 both dispersal and density-dependence. Results indicate that population growth rates  
13 generally increase with decreasing density, suggesting that encroachment is pulled by  
14 individuals at the low-density wave front, and the spatial population model predicts an  
15 encroachment rate of less than 2 cm per year. While the predicted rate of encroach-  
16 ment is consistent with observations over recent decades, it does not explain long-term  
17 creosotebush encroachment at the study site, suggesting that this process may occur in  
18 pulses when recruitment, seedling survival, or dispersal significantly exceed typical rates.  
19 Overall, our work demonstrates that individuals at low densities are likely the biggest  
20 contributors to creosotebush encroachment at this site, and that this encroachment is  
21 likely a process that occurs in large but infrequent bursts rather than at a steady pace.

## 22 Keywords

23 density-dependence, ecotones, woody encroachment, shrubs, integral projection model,  
24 grassland

---

<sup>1</sup>*I am not editing the abstract for now.*

## 25 Introduction

26 The recent and ongoing encroachment of shrubs and other woody plants into adjacent  
27 grasslands has caused significant vegetation changes across arid and semi-arid landscapes  
28 worldwide (Van Auken, 2000, 2009; Goslee et al., 2003; Gibbens et al., 2005; Parizek et al.,  
29 2002; Cabral et al., 2003; Trollope et al., 1989; Roques et al., 2001). The process of en-  
30 croachment generally involves increases in the number or density of woody plants in both  
31 time and space (Van Auken, 2000), which can drive shifts in plant community structure  
32 and alter ecosystem processes (Schlesinger et al., 1990; Ravi et al., 2009; Schlesinger  
33 and Pilmanis, 1998; Knapp et al., 2008). Other effects of encroachment include changes  
34 in ecosystem services (Reed et al., 2015; Kelleway et al., 2017), declines in biodiversity  
35 (Ratajczak et al., 2012; Sirami and Monadjem, 2012; Brandt et al., 2013), and economic  
36 losses in areas where the proliferation of shrubs adversely affects grazing land and pastoral  
37 production (Mugasi et al., 2000; Oba et al., 2000).

38 Woody plant encroachment can be studied through the lens of spatial population  
39 biology as a wave of individuals that may expand across space and over time (Kot et al.,  
40 1996; Neubert and Caswell, 2000; Wang et al., 2002; Pan and Lin, 2012). Theory pre-  
41 dicts that the speed of wave expansion depends on two processes: local demography and  
42 dispersal of propagules. First, local demographic processes include recruitment, survival,  
43 growth, and reproduction, which collectively determine the rate at which newly colonized  
44 locations increase in density and produce new propagules. Second, colonization events  
45 are driven by the spatial dispersal of propagules, which is commonly summarized as a  
46 probability distribution of dispersal distance, or “dispersal kernel”. The speed at which  
47 expansion waves move is highly dependent upon the shape of the dispersal kernel, espe-  
48 cially long-distance dispersal events in the tail of the distribution (Skarpaas and Shea,  
49 2007). Both demography and dispersal may depend on plant size, since larger plants  
50 often have improved demographic performance and release seeds from greater heights,

51 leading to longer dispersal distances (Nathan et al., 2011). Accounting for population  
52 structure, including size structure, may therefore be important for understanding and  
53 predicting wave expansion dynamics (Neubert and Caswell, 2000).

54 Theory predicts that the nature of conspecific density dependence is another critical  
55 feature of expansion dynamics but this is rarely studied in the context of woody plant  
56 encroachment. Expansion waves typically correspond to gradients of conspecific density  
57 – high in the back and low at the front – and demographic rates may be sensitive to  
58 density due to intraspecific interactions like competition or facilitation. If the demo-  
59 graphic effects of density are strictly negative due to competitive effects that increase  
60 with density then demographic performance is maximized as density goes to zero, at the  
61 leading edge of the wave. Under these conditions, the wave is “pulled” forward by indi-  
62 viduals at the low-density vanguard (Kot et al., 1996), and targeting these individuals  
63 and locations would be the most effective way to slow down or prevent encroachment  
64 (cite?). However, woody encroachment systems often involve positive feedbacks whereby  
65 shrub establishment modifies the environment in ways that facilitate further shrub re-  
66 cruitment. For example, woody plants can modify their micro-climates in ways that  
67 elevate nighttime minimum temperatures, promoting conspecific recruitment and sur-  
68 vival for freeze-sensitive species (D’Odorico et al., 2010; Huang et al., 2020). Such Allee  
69 effects (in the language of population biology) cause demographic rates to be maximized  
70 at higher densities behind the leading edge, which “push” the expansion forward, leading  
71 to qualitatively different dynamics (Kot et al., 1996; Taylor and Hastings, 2005; Sullivan  
72 et al., 2017; Lewis and Kareiva, 1993; Veit and Lewis, 1996; Keitt et al., 2001). Pushed  
73 expansion waves generally have different shapes (steeper density gradients) and slower  
74 speeds than pulled waves (Gandhi et al., 2016), and may require different strategies for  
75 managing or decelerating expansion (check Taylor and Hastings ref). The potential for  
76 positive feedbacks is well documented in woody encroachment systems but it remains  
77 unclear whether and how strongly these feedbacks decelerate shrub expansion and influ-

78   ence strategies for management of woody encroachment. Despite decades of work on this  
79   topic, we still do not know whether expansion waves of woody encroachment are pushed  
80   or pulled.

81       In this study, we linked woody plant encroachment to ecological theory for invasion  
82   waves, with the goals of understanding how seed dispersal and density-dependent demog-  
83   raphy drive encroachment, and determining whether the encroachment wave is pushed or  
84   pulled. Throughout the aridlands of the southwestern United States, shrub encroachment  
85   into grasslands is well documented (cite) but little is known about the dispersal and de-  
86   mographic processes that govern it. Our work focused on encroachment of creosotebush  
87   (*Larrea tridentata*) in the northern Chihuahuan Desert. Expansion of this species into  
88   grasslands over the past 150 years has been well documented, leading to decreased cover  
89   of *Bouteloua eriopoda*, the dominant foundation species of Chihuahuan desert grassland  
90   (Gardner, 1951; Buffington and Herbel, 1965; Gibbens et al., 2005). As in many woody  
91   encroachment systems, creosotebush expansion generates ecotones marking a transition  
92   from dense shrubland to open grassland, with a transition zone in between where shrubs  
93   can often be found interspersed among grasses (Fig. 1).

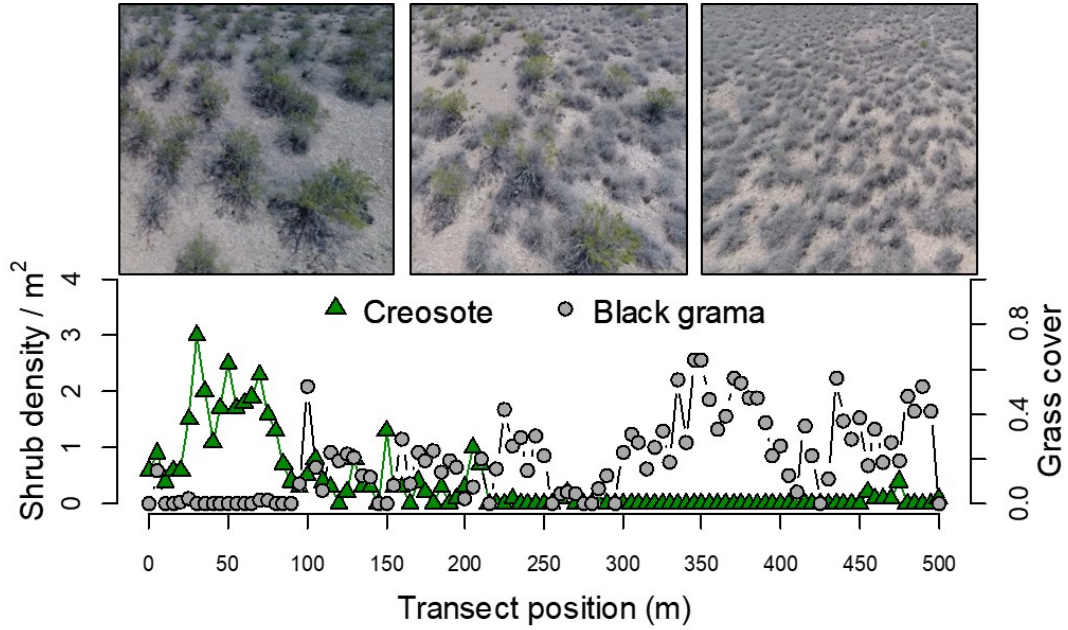


Figure 1: Caption.

94 Historically, creosotebush encroachment into grasslands is believed to have been  
 95 driven by a combination of factors including overgrazing, drought, variability in rain-  
 96 fall, and suppression of fire regimes Moreno-de las Heras et al. (2016). These shrubs  
 97 are also thought to further facilitate their own encroachment through positive feedbacks  
 98 (Grover and Musick, 1990; D’Odorico et al., 2012) by modifying their environment in ways  
 99 that favor continued growth and recruitment, such as the local micro-climate (D’Odorico  
 100 et al., 2010) and rates of soil erosion (Turnbull et al., 2010). Such positive feedback  
 101 also involve suppression of herbaceous competitors, reducing competition as well as the  
 102 amount of flammable biomass used to fuel the fires that keep creosotebush growth in  
 103 check (Van Auken, 2000). We hypothesized that, given potential for positive feedback  
 104 mechanisms, the rarity of conspecifics at the low-density encroachment front may depress  
 105 demographic performance and generate pushed-wave dynamics.

106 We used a combination of observational and experimental data from shrub ecotones

107 in central New Mexico to parameterize a spatial integral projection model (SIPM) that  
 108 predicts that speed of encroachment ( $m/yr$ ) resulting from lower-level demographic and  
 109 dispersal processes. Our data came from demographic surveys and experimental trans-  
 110 plants along replicate ecotone transects spanning a gradient of shrub density and seed  
 111 drop experiments to infer the properties of the dispersal kernel. We focused on wind  
 112 dispersal of seeds as a starting point, since little is known about the natural history  
 113 of dispersal in this system and the seeds lack rewards to attract animal dispersers. We  
 114 also used re-surveys of permanent transects as an independent measure of encroachment  
 115 that provided a benchmark against which to evaluate model predictions. The SIPM ac-  
 116 counts for size-structured demography of creosotebush, allows us to test whether shrub  
 117 expansion is pulled by the low-density front or pushed from the high-density core, and  
 118 identifies the local (demographic) and spatial (seed dispersal) life cycle transitions that  
 119 most strongly contribute to expansion speed<sup>2</sup>. We address the following specific ques-  
 120 tions:

- 121 1. What is the observed rate of creosotebush encroachment in recent past?
- 122 2. How do creosotebush size and conspecific density affect variation in demographic  
 123 vital rates (survival, growth, reproduction, and recruitment) along shrub encroach-  
 124 ment ecotones?
- 125 3. What is the wind dispersal kernel for this species and how far do seeds typically  
 126 travel by wind?
- 127 4. What is the predicted rate of expansion from the SIPM and what lower-level pro-  
 128 cesses most strongly govern the expansion speed?
- 129 5. Is encroachment pulled by the individuals at the front of the wave or pushed by  
 130 individuals behind it?

---

<sup>2</sup>*we will need to stay consistent with the language of encroachment/expansion/invasion. For now I am swictihg a lot.*

## 131 **Materials and methods**

### 132 **Study species**

133 Creosotebush *Larrea tridentata* is a perennial, drought-resistant shrub that is native to  
134 the arid and semiarid regions of the southwestern United States and northern Mexico.  
135 These shrubs are often found in valleys and on dunes and gentle slopes (Marshall, 1995).  
136 High-density areas of creosotebush consist largely of barren soil between plants due to  
137 the “islands of fertility” these shrubs create around themselves (Schlesinger et al., 1996;  
138 Reynolds et al., 1999), though lower-density areas will often contain grasses in the in-  
139 tershrub spaces (Fig. 1). In our northern Chihuahuan desert study region creosotebush  
140 reproduces sexually, with numerous small yellow flowers giving rise to highly pubescent  
141 spherical fruits several millimetres in diameter; these fruits consist of five carpels, each  
142 of which consists of a single seed. Seeds are dispersed from the parent plant by gravity  
143 and wind, with the possibility for seeds to also be blown across the soil surface or trans-  
144 ported by water runoff (Maddox and Carlquist, 1985). In other regions, this species also  
145 reproduces asexually and can give rise to long-lived clonal stands (Vasek, 1980), but this  
146 does not occur in our study region. The foliage is dark green, resinous, and unpalatable  
147 to most grazing and browsing animals (Mabry et al., 1978).

### 148 **Study site**

149 We conducted our experiments and censuses at the Sevilleta National Wildlife Refuge  
150 (SNWR), a Long-Term Ecological Research (LTER) site in central New Mexico. The  
151 refuge exists at the intersection of several eco-regions, including the Chihuahuan Desert  
152 and steppes of the Colorado Plateau. Annual precipitation is low at approximately  
153 250 mm, with the majority falling during the summer monsoon season from June to  
154 September.

155 Significant creosotebush encroachment at SNWR is believed to have last occurred



156 in the 1950's, with high shrub recruitment before and after a multi-year drought that  
157 caused a large loss in grass cover, setting the stage for creosotebush expansion (Moreno-  
158 de Las Heras et al., 2015; Moreno-de las Heras et al., 2016). The recruitment events  
159 that facilitate creosotebush expansion are thought to be highly episodic (Peters and Yao,  
160 2012). Given that creosotebush seedlings have been shown to establish around the time  
161 that late-summer heavy rainfall occurs (Boyd and Brum, 1983; Bowers et al., 2004),  
162 higher precipitation rates may be responsible for increased recruitment.

### 163 **Encroachment re-surveys**

164 We recorded shrub percent cover along two permanent 1000-m transects that spanned  
165 the shrub-grass ecotone, from high to low to near-zero shrub density. These surveys were  
166 conducted in summer 2001 and again in summer 2013 to document change in creosotebush  
167 abundance and spatial extent. At every 10 meters, shrub cover was recorded in nine cover  
168 classes (<1%, 1–4%, 5–10%, 10–25%, 25–33%, 33–50%, 50–75%, 75–95%, >95%). For  
169 visualization, we show midpoint values of these cover classes at each meter location for  
170 both transects and years.

### 171 **Demographic data**

#### 172 **Ecotone transects**

173 Collection of demographic data occurred during early June of every year from 2013-2017.  
174 This work was conducted at four sites in the eastern part of SNWR (one site was initiated  
175 in 2013 and the other three in 2014), with three transects at each site (different transects  
176 than those used for re-surveys). All transects were placed along a shrubland-grassland  
177 ecotone so that a full range of shrub densities was captured: each transect spanned  
178 core shrub areas, grassland with few shrubs, and the transition between them. Lengths  
179 of these transects varied from 200 to 600 m, determined by the strength of vegetation  
180 transition since “steep” transitions required less length to capture the full range of shrub

181 densities.

182 We quantified shrub density in 5-meter “windows” along each transect, including all  
183 plants within one meter of the transect on either side. Densities were quantified once for  
184 each transect (in 2013 or 2014) and were assumed to remain effectively constant for the  
185 duration of the study, a reasonable assumption for a species with very low recruitment  
186 and very high survival of established plants. Given the population’s size structure, we  
187 weighted the density of each window by the sizes of the plants, which we quantified as  
188 volume ( $\text{cm}^3$ ). Volume was calculated as that of an **elliptic**<sup>3</sup> cone:  $V_i = \frac{\pi h}{3} \frac{lw}{4}$  where  $l$ ,  
189  $w$ , and  $h$  are the maximum length, maximum width, and height, respectively. Maximum  
190 length and width were measured so that they were always perpendicular to each other,  
191 and height was measured from the base of the woody stem at the soil surface to the  
192 highest part of the shrub. The weighted density for a window was then expressed as  
193  $\log(\text{volume})$  summed over all plants in the window.

#### 194 **Observational census**

195 At 50-m intervals along each transect we tagged up to 10 plants for annual demographic  
196 census and recorded their local (5-m resolution) window so that we could connect indi-  
197 vidual demographic performance to local weighted density. These tagged shrubs were  
198 revisited every June and censused for survival (alive/dead), size (width, length, and  
199 height, as above), and reproduction (numbers of flowers and fruits). In instances where  
200 shrubs had large numbers of reproductive structures that would be difficult to reliably  
201 count (a large shrub may have many hundreds of flowers or fruits), we made counts on a  
202 fraction of the shrub and extrapolated to estimate whole-plant reproduction. Creosote-  
203 bush does not have a discrete reproductive season, instead producing flowers and fruits  
204 over much of the warm season. Our measurements of reproductive output are therefore  
205 conservative, and likely underestimate cumulative seed production for an entire transi-

---

<sup>3</sup>*I checked the code and actually this is not what we did.*

tion year. Each year, we also searched for new recruits within one  $m$  on either side of the transect. New recruits were tagged and added to the demographic census.

## Transplant experiment

We conducted a transplant experiment in 2015 to test how shrub density affects seedling survival. This approach complemented observational estimates of density dependence and filled in gaps for a part of the shrub life cycle that is rarely observed due to low recruitment. Seeds for the experiment were collected from plants in our study population in 2014. Seeds were germinated on Pro-Mix potting soil (Quakertown, PA) in Fall 2014 and seedlings were transferred to 3.8 cm-by-12.7 cm cylindrical containers and maintained in a greenhouse at Rice University. Seedlings were transported to SNWR and transplanted into our experimental design during July 27-31 2015. Transplant timing was intended to coincide with the start of the monsoon season, when most natural recruitment occurs.

The transplant experiment was conducted at the same four sites and three transects per site as the observational demographic census, where we knew weight shrub densities at 5-m window resolution. Along each transect we established 12 1-m by 1-m plots. Plots were intentionally placed to capture density variation: four plots were in windows with zero shrubs, four plots were placed in the top four highest-density windows, and the remaining four plots were randomly distributed among the remaining windows with weighted density greater than zero. Plots were placed in the middle of each 5-m window (at meter 2.5). Plots were divided into four 0.5-m by 0.5-m subplots. We divided each subplot into nine squares and recorded ground cover of each square as one of the following categories: bare, creosotebush, black grama (*B. eriopoda*), blue grama (*B. gracilis*), other grass, or “other”. Each subplot received one transplanted subplot, for a total of 48 transplants per transect, 144 transplants per site, and 576 transplants in the entire experiment. Each site was set up on a different day and there was a significant monsoon event after the third and before the fourth site. This resulted in differential mortality

that appears to be related to site (the soil was moist at the fourth site at the time of transplanting, which favored survival) but more likely reflects the timing of the monsoon event relative to planting. We revisited the transplant experiment on October 24, 2015 to survey mortality. After that first visit, transplants were censused along with the naturally occurring plants each June, following the methods described above.

## Demographic analysis

We fit statistical models to the demographic data and used AIC-based model selection to evaluate empirical support for alternative candidate models. The top statistical models were then used as the vital rate sub-models of the SIPM, so there is a strong connection between the statistical and population modeling, as is typical of integral projection modeling. Our analyses focused on the following demographic vital rates: survival, growth, probability of flowering, flower and fruit production, and seedling recruitment. All of these except recruitment were modeled as a function of plant size, and all of them included the possibility of density dependence, since we could connect the demographic performance of individual shrubs to the weighted density of their transect window.

The alternative hypotheses of pushed versus pulled wave expansion ultimately rest on how demographic vital rates, and the rate of population increase ( $\lambda$ ) derived from the combination of all vital rates, respond to density. We were particularly interested in whether demographic performance was maximized as local density goes to zero (pulled) or at non-zero densities behind the wave front (pushed). To flexibly model density dependence and detect non-monotonic responses, we used generalized additive models in the R package ‘mgcv’ (Wood, 2017). For each vital rate, we fit candidate models with or without a smooth term for local weighted density (among other possible covariates). To avoid over-fitting, we set the ‘gamma’ argument of `gam()` to 1.2, which increases the complexity penalty, results in smoother fits (Wood, 2017), and makes our approach more conservative. We pooled data across transition years for demographic analysis. All

models included the random effect of transect; we did not attempt to model both site and transect-within-site random effects due to the low numbers of each. All vital rate functions used the natural logarithm of volume ( $\text{cm}^3$ ) as the size variable and the sum  $\log(\text{volume})$  as the weighted density of a transect window.

**Growth** We modeled size in year  $t + 1$  as a Gaussian random variable. There were nine candidate models for growth (Table). The simplest model (1) defined the mean of size in year  $t + 1$  as a smooth function of size in year  $t$  and constant variance. Models (2) and (3) had constant variance but the mean included smooth terms for initial size and weighted density (2) or both smooth terms plus an interaction between initial size and weighted density (3). Models 4-6 had the same mean structure as 1-3 but defined the standard deviation of size in year  $t + 1$  as a smooth function of initial size. Models 7-9 mirrored 4-6 and additionally included a smooth term for weighted density in the standard deviation.

**Survival** We modeled survival or mortality in year  $t + 1$  as a Bernoulli random variable with three candidate models for survival probability. These included smooth terms for initial size in year  $t$  only (1), initial size and weighted density (3), and both smooth terms plus an interaction between initial size and weighted density. We analyzed survival of experimental transplants and observational census plants together in the same analyses, with a fixed effect of ‘transplant’ included in all candidate models. Since recruits and thus mortality events were both very rare in the observational survey, this approach allowed us to “borrow strength” over both data sets to generate a predictive function for size and possibly density -dependent survival while statistically accounting for differences between experimental and naturally occurring plants. Because we had additional, finer-grained cover data for the transplant experiment that we did not have for the observational census, we conducted an additional stand-alone analysis of transplant that explored the influence of covariates at multiple spatial scales (Appendix).

**Flowering and fruit production** We modeled shrub reproductive status (vegetative or flowering) in year  $t$  as a Bernoulli random variable with three candidate models for flowering probability. These included smooth terms for current size (in year  $t$ ) only (1), size and weighted density (3), and both smooth terms plus an interaction between size and weighted density. We modeled the reproductive output of flowering plants (the sum of flowerbuds, open flowers, and fruits) in year  $t$  as a negative binomial random variable. There were three candidate models for mean reproductive output that corresponded to the same three candidates for flowering probability.

**Recruitment** We modeled seedling recruitment in each transect window as a binomial random variable given the number of seeds produced in that window in the preceding year. To estimate window-level seed production, we used the best-fit models for flowering and fruit production and applied this to all plants in each window that we observed in our initial density surveys.

### **Integral Projection Model**

Collected demography data were then examined to investigate how weighted density and shrub volume affected four different demographic variables: survival, probability of flowering (i.e. producing at least one flower or fruit), annual growth, and number of reproductive structures. Each of these demographic variables was fit to a different mixed-effects model through maximum likelihood. Both survival and probability of flowering were each fit to generalised linear mixed-effects models using a binomial response and a logit link function. Annual growth was defined as  $\ln(V_{t+1}/V_t)$  where  $V_{t+1}$  and  $V_t$  are the shrub volumes in the current and previous years, respectively, and was then fit to a linear mixed-effects model. The number of reproductive structures was defined as the natural logarithm of the sum of fruits and flowers on the entire shrub and was fit to a linear mixed-effects model as well. To construct these models, all of the equations listed in

Table 1 were first fit to each of the four demographic variables, with each equation using volume and standardised density as predictors while also treating the unique transect in which each shrub was located as a random effect. After these equations were fit to the data, all eight equations for each demographic variable were ranked based on their value of the Akaike information criterion (AIC) and weighted based on their quality so that better-fitting models had a higher weight. Then, coefficients of the same type were averaged between all eight models for each demographic variable using a weighted mean corresponding to model quality in order to generate an average model. All four average models have the general form

$$R = \beta_1 v + \beta_2 d + \beta_3 d^2 + \beta_4 vd + \beta_5 vd^2 + \epsilon \quad (1)$$

where  $R$  is the response variable,  $v$  and  $d$  are the volume and density,  $\epsilon$  is a random transect effect, and  $\beta$  is the coefficient for each type of term.

The effect of density dependence on the probability of recruitment from seeds was also modelled. For every year, the sum of seeds produced the prior year was calculated for each 5-m subsection, and then probability of recruitment was calculated as the number of recruits observed in each 5-m subsection divided by that number of seeds. For any subsection in which seeds were not found, a count of seeds was estimated based on the number of seeds in a subsection of similar weighted density; this was done to avoid creating any undefined values of recruitment probability. Both linear and quadratic models using only weighted density as a predictor were fit to the distribution of recruitment probabilities, though the linear model was ultimately used because it had a higher AIC value.

## 331 Dispersal modelling

332 Dispersal kernels were calculated using the WALD, or Wald analytical long-distance  
 333 dispersal, model that uses a mechanistic approach to predict dispersal patterns of plant  
 334 propagules by wind. The WALD model, which is largely based in fluid dynamics, can  
 335 serve as a good approximation of empirically-determined dispersal kernels (Katul et al.,  
 336 2005; Skarpaas and Shea, 2007) and may be used when empirical dispersal data is not  
 337 readily available. Under the assumptions that wind turbulence is low, wind flow is  
 338 vertically homogenous, and terminal velocity is achieved immediately upon seed release,  
 339 the WALD model simplifies a Lagrangian stochastic model to create a dispersal kernel  
 340 that estimates the likelihood a propagule will travel a given distance (Katul et al., 2005).  
 341 This dispersal kernel takes the form of the inverse Gaussian distribution

$$342 \quad p(r) = \left( \frac{\lambda'}{2\pi r^3} \right)^{\frac{1}{2}} \exp \left[ -\frac{\lambda'(r - \mu')^2}{2\mu'^2 r} \right] \quad (2)$$

343 that is a slight adaptation from equation 5b in Katul et al. (2005), using  $r$  to denote  
 344 dispersal distance. Here,  $\lambda'$  is the location parameter and  $\mu'$  is the scale parameter,  
 345 which depend on environmental and plant-specific properties of the study system. The  
 346 location and scale parameters are defined as  $\lambda' = (H/\sigma)^2$  and  $\mu' = HU/F$ ; these are  
 347 functions of the height  $H$  of seed release, wind speed  $U$  at seed release height, seed  
 348 terminal velocity  $F$ , and the turbulent flow parameter  $\sigma$  that depends on both wind  
 349 speed and local vegetation roughness.

350 In order to create the dispersal kernel, we first take the wind speeds at measure-  
 351 ment height  $z_m$  and correct them to find wind speed  $U$  for any height  $H$  by using the  
 352 logarithmic wind profile

$$353 \quad U = \frac{1}{H} \int_{d+z_0}^H \frac{u^*}{K} \log \left( \frac{z-d}{z_0} \right) dz \quad (3)$$



354 given in Bullock et al. (2012) equation 6, with the notation slightly modified. Here,  $z$   
 355 is the height above the ground,  $K$  is the von Karman constant, and  $u^*$  is the friction  
 356 velocity. The zero-plane displacement  $d$  and roughness length  $z_0$  are surface roughness  
 357 parameters that, for a grass canopy height  $h$  above the ground, are approximated by  
 358  $d \approx 0.7h$  and  $z_0 \approx 0.1h$ . These estimates are from Raupach (1994) for a canopy area  
 359 index  $\Lambda = 1$  in which the sum of grass canopy elements is equal to the unit area being  
 360 measured. A 0.15 m grass height at the study site gives  $d = 0.105$  and  $z_0$ , which are  
 361 suitable approximations for grassland (Wiernga, 1993). Calculations of  $u^*$  were done  
 362 using equation A2 from Skarpaas and Shea (2007), in which

$$363 \quad u^* = KU_m \left[ \log \left( \frac{z_m - d}{z_0} \right) \right]^{-1} \quad (4)$$

364 and  $U_m$  is the mean wind velocity at the measurement height  $z_m$ . Values for the turbulent  
 365 flow parameter  $\sigma$  were then calculated using the estimate made by Skarpaas and Shea  
 366 (2007) in their equation A4, where

$$367 \quad \sigma = 2A_w^2 \sqrt{\frac{K(z - d)u^*}{C_0 U}} \quad (5)$$

368 and  $C_0$  is the Kolmogorov constant.  $A_w$  is a constant that relates vertical turbulence  
 369 to friction velocity and is approximately equal to 1.3 under the assumptions of above-  
 370 canopy flow made by Skarpaas and Shea (2007), based off calculations from Hsieh and  
 371 Katul (1997). In addition, the assumption that  $z = H$  was made in order to make the  
 372 calculation of  $\sigma$  more feasible.

373 The values from the previous three equations give us the necessary information to  
 374 calculate  $\mu'$  and  $\lambda'$ , thus allowing us to create the WALD distribution  $p(r)$ . However, the  
 375 base WALD model does not take into account variation in wind speeds or seed terminal  
 376 velocities, which limits its applicability in systems where such variation is present. In  
 377 order to account for this variation, we integrate the WALD model over distributions these

378 two variables using the same method as Skarpaas and Shea (2007). The WALD model  
 379 assumes seed release from a single point source, though, which is not realistic for a shrub;  
 380 because seeds are released across the entire height of the shrub rather than from a point  
 381 source,  $p(r)$  was also integrated across the uniform distribution from the grass canopy  
 382 height to the shrub height. Thus, under the assumptions that the height at which a  
 383 seed is located does not affect its probability of being released and that seeds are evenly  
 384 distributed throughout the shrub, this gives the dispersal kernel  $K(r)$ , where

$$385 \quad K(r) = \iiint p(F)p(U)p(z)p(r) dF dU dz \quad (6)$$

386 and  $p(F)$  and  $p(U)$  are the PDFs of the terminal velocity  $F$  and wind speed  $U$ , respec-  
 387 tively, and  $p(z)$  is the uniform distribution from  $h$  to  $H$ .

388 The distribution  $p(F)$  in the integral above was constructed using experimentally  
 389 determined seed terminal velocities. This was done by using a high-speed camera and  
 390 motion tracking software to determine position as a function of time, and then using the  
 391 Levenberg-Marquardt algorithm to solve a quadratic-drag equation of motion for  $F$ . Be-  
 392 fore seeds were released, they were dried and then dyed with yellow fluorescent powder,  
 393 and then put against a black background to improve visibility and make tracking easier.  
 394 While the powder added mass to the seeds, this added mass only yielded an approxi-  
 395 mately 2.5% increase and was thus negligible, likely having little effect on their terminal  
 396 velocities. Measurements were conducted for 48 seeds that were randomly chosen from a  
 397 seed pool derived from different plants, and then an empirical PDF of terminal velocities  
 398 was constructed using the data. Constructing  $p(U)$  involved creating an empirical PDF  
 399 of hourly wind speeds at Five Points, the site closest to the 12 transects being used,  
 400 that were obtained from meteorological data collected at the Sevilleta National Wildlife  
 401 Refuge from 1988 to 2010. We did not weight  $p(U)$  and assumed that the probability  
 402 seed release from the shrub is the same regardless of wind speed.

## Spatial integral projection model

Given that the shrub population at this site is approximately homogeneous perpendicular to the direction of encroachment, expansion is modelled as a wave moving in one dimension. A spatial integral projection model (SIPM) is used to estimate the speed at which encroachment occurs; such a model incorporates the effects of variation in traits like plant size that stage-structured models, such as those described in Neubert and Caswell (2000), do not capture. According to Jongejans et al. (2011), a general SIPM can be formulated as

$$\mathbf{n}(x_2, z_2, t + 1) = \iint \tilde{K}(x_2, x_1, z_2, z_1) \mathbf{n}(x_1, z_1, t) dx_1 dz_1 \quad (7)$$

where  $x_1$  and  $x_2$  are locations of individuals of a particular size before and after one unit of time, and  $z_1$  and  $z_2$  are the respective sizes. The vector  $\mathbf{n}$  indicates the population density of each size, and  $\tilde{K}$  is a kernel that combines dispersal with demography. Though this SIPM represents a continuous spectrum of shrub sizes and densities, it was implemented by discretising the above integral with a 200 x 200 matrix, as this makes calculations significantly more tractable.

Movement of the wave is determined by the components of the combined dispersal/demography kernel  $\tilde{K}$ , which is of the same form as that used in Jongejans et al. (2011). Here,

$$\tilde{K}(x_2, x_1, z_2, z_1) = K(x_2 - x_1)Q(z_2 - z_1) + \delta(x_2 - x_1)G(z_2 - z_1) \quad (8)$$

and  $K$  is the dispersal kernel,  $Q$  a reproduction function,  $G$  a growth function, and  $\delta$  the Dirac delta function.  $G$  is derived from the model for annual growth ratio, and  $Q$  is derived from the reproductive structures model as well as other factors including number of seeds per reproductive structure, probability of recruitment from seed, and recruit

size. Both  $G$  and  $Q$  give the probability of transition between sizes; in the case of  $G$ , this is the probability of growing from one specific size to another, and in the case of  $Q$  the probability that an individual of a specific size produces a recruit of a specific size. The product of  $K$  and  $Q$  represents the production and dispersal of motile propagules, while the product of  $G$  and  $\delta$  represents the growth of sessile individuals.

Given growth function  $G$  and the reproduction function  $Q$ , the speed of the moving wave can be calculated as

$$c^* = \min_{s>0} \left[ \frac{1}{s} \ln(\rho_s) \right] \quad (9)$$

where  $s$  is the wave shape parameter and  $\rho_s$  is the dominant eigenvalue of the kernel  $\mathbf{H}_s$  (Jongejans et al., 2011). This estimate for the wavespeed is valid under the assumption that population growth decreases monotonically as conspecific density increases, with the highest rates of growth occurring at the lowest population densities (Lewis et al., 2006). The kernel  $\mathbf{H}_s$  is defined as

$$\mathbf{H}_s = M(s)Q(z_2 - z_1) + G(z_2 - z_1) \quad (10)$$

where  $M(s)$  is the moment-generating function of the dispersal kernel (Jongejans et al., 2011). For one-dimensional dispersal, this moment-generating function can be estimated as

$$M(s) = \frac{1}{N} \sum_{i=1}^n I_0(sr_i) \quad (11)$$

where  $r$  is the dispersal distance for each observation, and  $I_0$  is the modified Bessel function of the first kind and zeroth order (Skarpaas and Shea, 2007). In order to obtain  $M$ , numerous dispersal distances were simulated from the dispersal kernel  $K(r)$  described in the previous section, with over 2000 replications for each shrub height increment of 1 cm. This was performed over the range from the lowest possible dispersal height to the maximum shrub height. Once  $M(s)$  was obtained for dispersal at each shrub height,  $\mathbf{H}_s$

450 and  $c^*$  were calculated for each value of  $s$ ; this was done for values of  $s$  ranging from 0  
451 to 2, as it is this range in which  $c^*$  occurs.

452 Estimates of the wavespeed were bootstrapped for a total of 1000 replicates. Each  
453 bootstrap replicate recreated size- and density-dependent demographic models using 80%  
454 resampling on the original demographic data, and recreated dispersal kernels also using  
455 80% resampling on the wind speeds and seed terminal velocities. Between replicates,  
456 the structure of the demographic models was kept constant, though coefficient estimates  
457 were not; this approach, while effectively ignoring model uncertainty, has the benefit of  
458 increasing computational efficiency, which is especially useful given the time-consuming  
459 nature of numerically estimating the many dispersal kernels used in the model.

## 460 Results

### 461 Encroachment re-surveys

462 Figure 2.

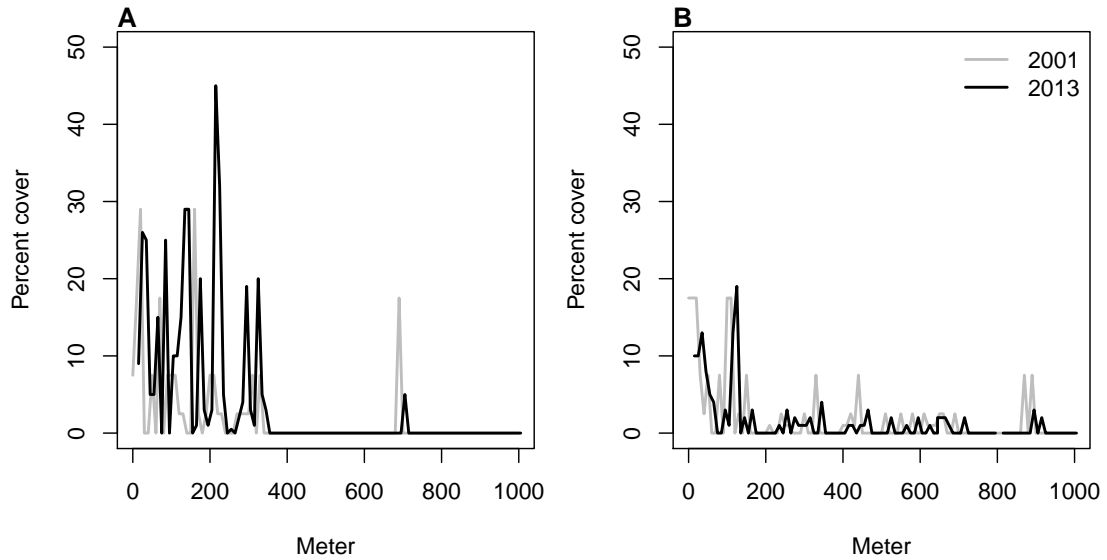


Figure 2: Re-surveys of shrub cover along two permanent transects (A,B) surveyed in 2001 and 2013.

463 The speed of encroachment at the study site as estimated by the SIPM is rather  
 464 slow; as can be seen in Figure 3, the low-density wavefront moves at approximately  
 465 0.5 cm/yr under normal conditions and at 1 cm/yr under the best seedling survival  
 466 conditions observed in the dataset. These improved conditions were observed due to  
 467 above-average rainfall that occurred after greenhouse-grown seedlings were transplanted  
 468 to the site. Population growth in this low-density region of the moving wave is also low,  
 469 with a geometric growth rate of  $\lambda \approx 1.006$  and even lower rates of growth the higher-  
 470 density regions behind; in the higher-survival scenario the maximum rate increases to  
 471  $\lambda \approx 1.013$ , with growth still decreasing as density increases. For both scenarios, the  
 472 decrease in population growth rate with increasing density was monotonic across the  
 473 range of observed standardised densities, as is shown in Figure 3. This suggests that  
 474 an Allee effect is likely not present in this population, as the highest rate of population  
 475 growth is found at the lowest density vanguard of the encroaching population. Thus, the  
 476 conditions necessary for equation 9 to be valid are satisfied, and these wavespeeds are  
 477 applicable for a pulled-wave scenario in which no Allee effects are present.

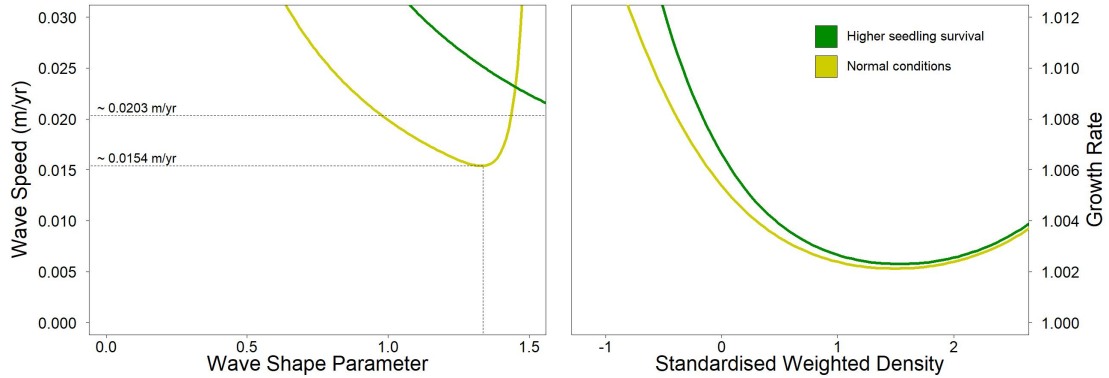


Figure 3: Estimated encroachment wave speeds (left) and geometric rates of population growth (right) for higher post-rainfall seedling survival and normal conditions.

478 As the speed of encroachment is quite limited, so is the extent of wind dispersal.  
 479 Long distance dispersal events, while more common for taller shrubs than their shorter

counterparts, are still uncommon overall. For the tallest shrub height of 1.98 m, only 0.32% of propagules exceed a dispersal distance of 5 m, and 0.02% exceed 10 m. At 1 m, or approximately half the tallest shrub height, long distance dispersal is even less likely, with 0.0046% of propagules exceeding a dispersal distance of 5 m and 0.0009% exceeding 10 m. Given that the median shrub height is only 0.64 m, the occurrence of long-distance wind dispersal in most of the shrub population is highly improbable, and the few instances in which it occurs will only be limited to the tallest shrubs. Thus, as Figure 4 demonstrates, shorter dispersal distances dominate; even for the tallest shrub, 81% of seeds fall within only a metre of the plant, and this percentage increases as shrub height decreases. Dispersal kernels have their highest probability density at dispersal distances between 2 and 8 cm from the shrub; here, as shrub height increases, the most probable dispersal distance slightly increases while maximum probability density decreases. Regardless of the shrub height, most dispersal will occur very close to the plant, though increases in shrub height dramatically increase the likelihood of dispersal at longer distances. It is clear that the shape of the height-dependent dispersal kernel  $K(r)$  varies greatly among the shrub population given the large range of shrub heights observed; shrubs at lower heights have more slender kernels with most of the seeds dispersing closer to the plant, while taller shrubs have kernels with much fatter tails and are more capable of longer-distance dispersal.

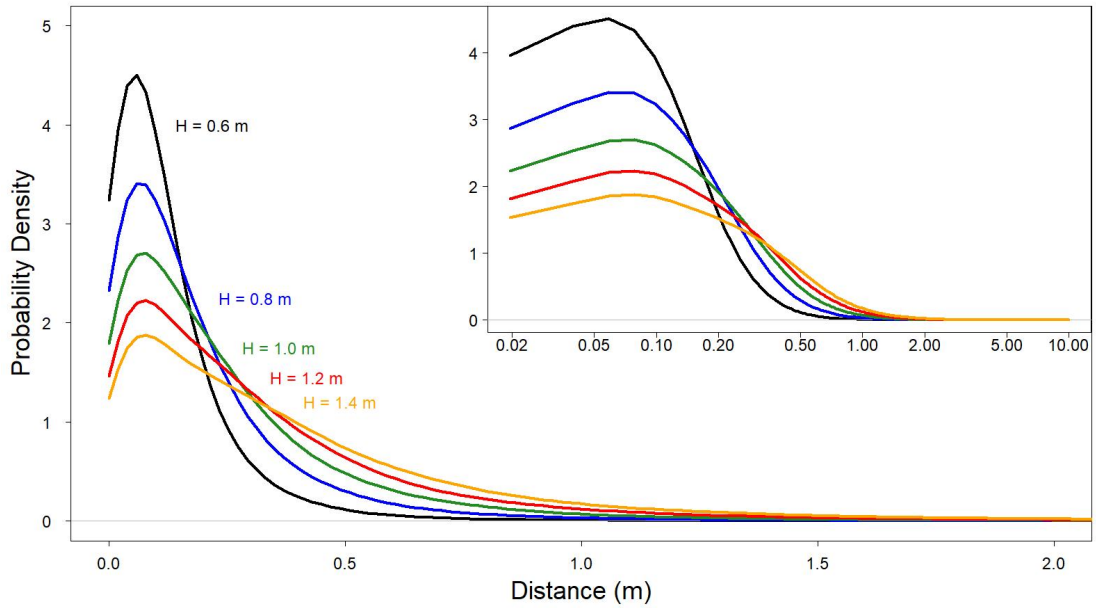


Figure 4: Dispersal kernels, with each colour representing a selected shrub height. The inset plot is the same as the large plot, though with a logarithmic x-axis to more easily show differences in dispersal probability at smaller distances.

499 Density and size dependence are evident in all 4 of the demographic rates, with  
 500 coefficients for each model displayed in Table 2. For growth, reproduction, and survival,  
 501 density dependence is mostly negative and monotonic; this is not the case for probability  
 502 of flowering, where shrub size seems to be more important than the effects of density alone  
 503 and suggests that larger shrubs have a higher probability of flowering than their smaller  
 504 counterparts. This, along with size and density dependence in growth and reproduction,  
 505 is shown in Figure 5. Size dependence is positive for reproduction, as would be expected  
 506 since larger plants typically produce more flowers and fruits. However, annual growth  
 507 decreases as size increases; this could be in part due to the annual growth in this study  
 508 being quantified as a proportion relative to the shrub's initial size. While larger shrubs  
 509 may produce more plant material over a year in terms of absolute volume, smaller shrubs  
 510 produce less but can still have higher annual growth in terms of the percentage of volume



511 added relative to their initial volume. When compared to density, shrub size is a much  
512 stronger predictor of survival, with significant differences in mortality rates depending on  
513 shrub size. For small shrubs, mortality is exceptionally high, and increases in volume for  
514 these shrubs only slightly increase the likelihood of survival. However, after shrubs reach  
515 a logarithmic volume of approximately 7.3, they are almost guaranteed to survive, with  
516 survival rates near 100% persisting regardless of any further size increases. Interestingly,  
517 though most recruits were found at lower densities, the probability of recruitment from  
518 seed displays positive density dependence; the probability of recruitment was still very  
519 low, though, with a baseline rate of approximately 2 recruits per 10,000 seeds.

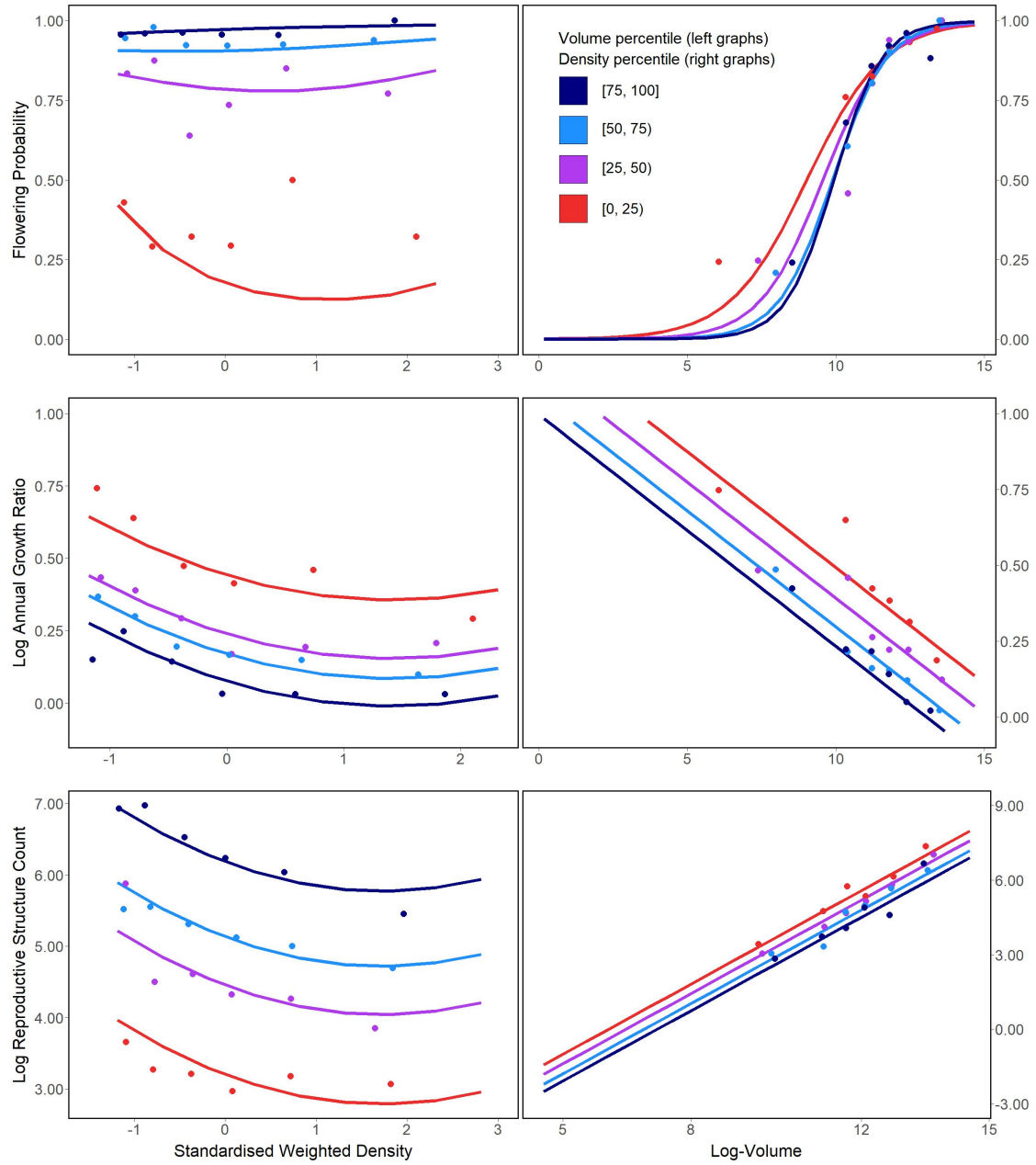


Figure 5: Flowering probability (top row), log annual growth ratio (centre row), and log reproductive structure count (bottom row) at all four sampling sites. In the left column of graphs, the three response variables are shown as a function of density for each of four volume quartiles, with each quartile containing six density bins; in the right column, the opposite occurs, with response variables shown as functions of four volume quartiles that each contain six density bins. Graphs quantifying the number of reproductive structures include data only on plants that flowered.

## Discussion

The slow movement of the encroaching creosotebush wave at the Sevilleta LTER site can likely be contributed to a combination of three factors: short dispersal distances with extremely limited long-distance dispersal events, very low probability of recruitment from seed, and high seedling mortality. These three barriers, when combined, form a formidable challenge to the establishment of new shrubs at the low-density front of the wave. First, a seed must travel far enough to avoid competition with the parent shrub, which is unlikely given the dispersal kernels shown in Figure 2. Even if the seed manages to be dispersed this far, its chances of becoming a seedling are low. Caching and consumption by seed-eaters such as a variety of seed-harvesting ants (Whitford, 1978; Whitford et al., 1980; Lei, 1999) and the kangaroo rat *Dipodomys merriami* (Chew and Chew, 1970) decreases the amount of seeds available for germination. However, reduction in germination caused by destruction of seeds may be partly mitigated by the more favourable germination conditions that these seeds can experience when cached underground (Chew and Chew, 1970). Many of the remaining seeds will still fail to germinate, and in the unlikely event that germination does occur, seedlings will likely die given the high rates of mortality observed in smaller shrubs. Such high rates of creosotebush seedling mortality have been observed in other studies as well (Boyd and Brum, 1983; Bowers et al., 2004), probably due to a combination of herbivory, competition, and abiotic stresses.

However, as low as they are, the wavespeed estimates given in this paper are still conservative estimates for reasons mostly related to dispersal. First, it is important to note that the dispersal kernels used here, while they account for variation in factors such as wind speed and terminal velocity, may underestimate the distances that shrub propagules travel. Because the WALD model assumes that terminal velocity is reached immediately upon seed release, seeds in the estimate thus take a shorter time to fall

546 and have less time to be transported by wind, and the true frequency of long-distance  
547 dispersal events may thus be greater than what is estimated here. Second, dispersal at the  
548 study site could occur through additional mechanisms other than wind. For example,  
549 secondary dispersal through runoff from significant rainfall events can transport seeds  
550 (Thompson et al., 2014), and given that long-distance dispersal by bird and subsequent  
551 species divergence is thought to be responsible for creosotebush being in North America  
552 in the first place (Wells and Hunziker, 1976), short-distance dispersal by other animals  
553 at the study site likely occurs. As mentioned above, seeds are transported by seed-  
554 harvesting ants and granivorous mammals, where they are often stored in caches that  
555 can be appreciable distances from the parent shrubs. Whether transportation occurs via  
556 ant or rodent, creosotebush seeds can be moved significantly further than wind alone  
557 can, though many of these seeds are eventually consumed.

558 Despite the more conservative estimates our model yields, the estimated rate of dis-  
559 persal in creosotebush populations at the Sevilleta National Wildlife Refuge is consistent  
560 with observations from the past 50-60 years, as creosotebush expansion during this time  
561 has been minimal (Moreno-de las Heras et al., 2016). However, it cannot explain the  
562 long-term increases in creosotebush cover at the study site, as total encroachment over  
563 the past 150 years is much greater than what would be expected given the encroachment  
564 rates derived by our models. Such a discrepancy is likely due to much of the expansion  
565 occurring in an episodic fashion, with short times during which rapid encroachment oc-  
566 curs due to favourable environmental conditions. This could be due in part to seedling  
567 recruitment, which is a factor that strongly limits creosotebush expansion, being rare  
568 and episodic. For example, Allen et al. (2008) estimate that a major recruitment event  
569 occurred at this site in the 1950s, which is supported by photographic evidence from  
570 Milne et al. (2003) of a drought-driven expansion during this time. Moreno-de las Heras  
571 et al. (2016) estimate that after this expansion, several smaller creosotebush recruitment  
572 events occurred in decadal episodes. However, such events can be highly localised and

573 may not necessarily occur at the low-density front of encroachment, which could explain  
574 how these recruitment events can still coexist with lack of encroachment in the recent  
575 past.

576 Overall, our observations and model highlight three aspects of creosotebush encroach-  
577 ment that should be the focus of future studies seeking to obtain better estimates of  
578 encroachment rates. First, negative density dependence in survival, growth, and repro-  
579 duction is demonstrated, along with size dependence. The clear dependence on size and  
580 conspecific density suggests that they both should be considered when estimating cre-  
581 osotebush expansion and quantifying the demographic variation that contributes to it.  
582 Second, wind dispersal in these shrubs is quite limited; though the dispersal kernels seen  
583 here are typical in the sense that they are characterised by high near-plant dispersal and  
584 exceptionally low long-distance dispersal, the scale across which such dispersal occurs  
585 is small, with most seeds landing within only 1 m of the shrub. Wind dispersal alone  
586 may be an underestimate of the true amount of dispersal occurring, and future work  
587 should seek to incorporate the effects of dispersal by runoff and animals so that a more  
588 representative model of total dispersal can be obtained. Finally, encroachment is slow or  
589 even stagnates, but only most of the time. Though our encroachment speed estimates  
590 are representative of creosotebush populations for most years, the significant expansion  
591 seen over larger time scales suggests that there is episodic expansion in other years; while  
592 our model is consistent with the recent stagnation in creosotebush encroachment at the  
593 Sevilleta LTER site, a model that also includes interannual variability in factors such  
594 as survival and recruitment would be able to better account for instances of episodic  
595 population expansion that are characteristic of this location.

## 596 Acknowledgements

## 597 Author contributions

## 598 Data accessibility

## 599 References

- 600 Allen, A., W. Pockman, C. Restrepo, and B. Milne. 2008. Allometry, growth and  
601 population regulation of the desert shrub *Larrea tridentata*. *Functional Ecology* pages  
602 197–204.
- 603 Bowers, J. E., R. M. Turner, and T. L. Burgess. 2004. Temporal and spatial patterns in  
604 emergence and early survival of perennial plants in the Sonoran Desert. *Plant Ecology*  
605 **172**:107–119.
- 606 Boyd, R. S., and G. D. Brum. 1983. Postdispersal reproductive biology of a Mojave Desert  
607 population of *Larrea tridentata* (Zygophyllaceae). *American Midland Naturalist* pages  
608 25–36.
- 609 Brandt, J. S., M. A. Haynes, T. Kuemmerle, D. M. Waller, and V. C. Radeloff. 2013.  
610 Regime shift on the roof of the world: Alpine meadows converting to shrublands in  
611 the southern Himalayas. *Biological Conservation* **158**:116–127.
- 612 Buffington, L. C., and C. H. Herbel. 1965. Vegetational changes on a semidesert grassland  
613 range from 1858 to 1963. *Ecological monographs* **35**:139–164.
- 614 Bullock, J. M., S. M. White, C. Prudhomme, C. Tansey, R. Perea, and D. A. Hooftman.  
615 2012. Modelling spread of British wind-dispersed plants under future wind speeds in  
616 a changing climate. *Journal of Ecology* **100**:104–115.

617 Cabral, A., J. De Miguel, A. Rescia, M. Schmitz, and F. Pineda. 2003. Shrub encroach-  
618 ment in Argentinean savannas. *Journal of Vegetation Science* **14**:145–152.

619 Chew, R. M., and A. E. Chew. 1970. Energy relationships of the mammals of a desert  
620 shrub (*Larrea tridentata*) community. *Ecological Monographs* pages 2–21.

621 D’Odorico, P., J. D. Fuentes, W. T. Pockman, S. L. Collins, Y. He, J. S. Medeiros,  
622 S. DeWekker, and M. E. Litvak. 2010. Positive feedback between microclimate and  
623 shrub encroachment in the northern Chihuahuan desert. *Ecosphere* **1**:1–11.

624 D’Odorico, P., G. S. Okin, and B. T. Bestelmeyer. 2012. A synthetic review of feedbacks  
625 and drivers of shrub encroachment in arid grasslands. *Ecohydrology* **5**:520–530.

626 Gandhi, S. R., E. A. Yurtsev, K. S. Korolev, and J. Gore. 2016. Range expansions  
627 transition from pulled to pushed waves as growth becomes more cooperative in an  
628 experimental microbial population. *Proceedings of the National Academy of Sciences*  
629 **113**:6922–6927.

630 Gardner, J. L. 1951. Vegetation of the creosotebush area of the Rio Grande Valley in  
631 New Mexico. *Ecological Monographs* **21**:379–403.

632 Gibbens, R., R. McNeely, K. Havstad, R. Beck, and B. Nolen. 2005. Vegetation changes  
633 in the Jornada Basin from 1858 to 1998. *Journal of Arid Environments* **61**:651–668.

634 Goslee, S., K. Havstad, D. Peters, A. Rango, and W. Schlesinger. 2003. High-resolution  
635 images reveal rate and pattern of shrub encroachment over six decades in New Mexico,  
636 USA. *Journal of Arid Environments* **54**:755–767.

637 Grover, H. D., and H. B. Musick. 1990. Shrubland encroachment in southern New Mexico,  
638 USA: an analysis of desertification processes in the American Southwest. *Climatic*  
639 *change* **17**:305–330.

- 640 Hsieh, C.-I., and G. G. Katul. 1997. Dissipation methods, Taylor’s hypothesis, and  
641 stability correction functions in the atmospheric surface layer. *Journal of Geophysical*  
642 *Research: Atmospheres* **102**:16391–16405.
- 643 Huang, H., L. D. Anderegg, T. E. Dawson, S. Mote, and P. D’Odorico. 2020. Crit-  
644 ical transition to woody plant dominance through microclimate feedbacks in North  
645 American coastal ecosystems. *Ecology* **101**:e03107.
- 646 Jongejans, E., K. Shea, O. Skarpaas, D. Kelly, and S. P. Ellner. 2011. Importance of  
647 individual and environmental variation for invasive species spread: a spatial integral  
648 projection model. *Ecology* **92**:86–97.
- 649 Katul, G., A. Porporato, R. Nathan, M. Siqueira, M. Soons, D. Poggi, H. Horn, and  
650 S. A. Levin. 2005. Mechanistic analytical models for long-distance seed dispersal by  
651 wind. *The American Naturalist* **166**:368–381.
- 652 Keitt, T. H., M. A. Lewis, and R. D. Holt. 2001. Allee effects, invasion pinning, and  
653 species’ borders. *The American Naturalist* **157**:203–216.
- 654 Kelleway, J. J., K. Cavanaugh, K. Rogers, I. C. Feller, E. Ens, C. Doughty, and N. Sain-  
655 tilan. 2017. Review of the ecosystem service implications of mangrove encroachment  
656 into salt marshes. *Global Change Biology* **23**:3967–3983.
- 657 Knapp, A. K., J. M. Briggs, S. L. Collins, S. R. Archer, M. S. BRET-HARTE, B. E.  
658 Ewers, D. P. Peters, D. R. Young, G. R. Shaver, E. Pendall, et al. 2008. Shrub  
659 encroachment in North American grasslands: shifts in growth form dominance rapidly  
660 alters control of ecosystem carbon inputs. *Global Change Biology* **14**:615–623.
- 661 Kot, M., M. A. Lewis, and P. van den Driessche. 1996. Dispersal data and the spread of  
662 invading organisms. *Ecology* **77**:2027–2042.



663 Lei, S. A. 1999. Ecological impacts of *Pogonomyrmex* on woody vegetation of a *Larrea*-  
 664 *Ambrosia* shrubland. *The Great Basin Naturalist* pages 281–284.

665 Lewis, M., and P. Kareiva. 1993. Allee dynamics and the spread of invading organisms.  
 666 *Theoretical Population Biology* **43**:141–158.

667 Lewis, M. A., M. G. Neubert, H. Caswell, J. S. Clark, and K. Shea, 2006. A guide  
 668 to calculating discrete-time invasion rates from data. Pages 169–192 *in* *Conceptual*  
 669 *ecology and invasion biology: reciprocal approaches to nature*. Springer.

670 Mabry, T. J., J. H. Hunziker, D. Difeo Jr, et al. 1978. Creosote bush: biology and  
 671 chemistry of *Larrea* in New World deserts. Dowden, Hutchinson & Ross, Inc.

672 Maddox, J. C., and S. Carlquist. 1985. Wind dispersal in Californian desert plants:  
 673 experimental studies and conceptual considerations. *Aliso: A Journal of Systematic*  
 674 *and Evolutionary Botany* **11**:77–96.

675 Marshall, A. K., 1995. *Larrea tridentata*. URL [https://www.fs.fed.us/database/](https://www.fs.fed.us/database/feis/plants/shrub/lartri/all.html#8)  
 676 [feis/plants/shrub/lartri/all.html#8](https://www.fs.fed.us/database/feis/plants/shrub/lartri/all.html#8).

677 Milne, B. T., D. I. Moore, J. L. Betancourt, J. A. Parks, T. W. Swetnam, R. R. Par-  
 678 menter, and W. T. Pockman. 2003. Multidecadal drought cycles in south-central New  
 679 Mexico: Patterns and consequences. Oxford University Press: New York, NY.

680 Moreno-de Las Heras, M., R. Díaz-Sierra, L. Turnbull, and J. Wainwright. 2015. Assess-  
 681 ing vegetation structure and ANPP dynamics in a grassland–shrubland Chihuahuan  
 682 ecotone using NDVI–rainfall relationships. *Biogeosciences* **12**:2907–2925.

683 Moreno-de las Heras, M., L. Turnbull, and J. Wainwright. 2016. Seed-bank structure  
 684 and plant-recruitment conditions regulate the dynamics of a grassland-shrubland Chi-  
 685 huahuan ecotone. *Ecology* **97**:2303–2318.

- 686 Mugasi, S., E. Sabiiti, and B. Tayebwa. 2000. The economic implications of bush  
687 encroachment on livestock farming in rangelands of Uganda. *African Journal of Range*  
688 *and Forage Science* **17**:64–69.
- 689 Nathan, R., G. G. Katul, G. Bohrer, A. Kupařinen, M. B. Soons, S. E. Thompson,  
690 A. Trakhtenbrot, and H. S. Horn. 2011. Mechanistic models of seed dispersal by wind.  
691 *Theoretical Ecology* **4**:113–132.
- 692 Neubert, M. G., and H. Caswell. 2000. Demography and dispersal: calculation and  
693 sensitivity analysis of invasion speed for structured populations. *Ecology* **81**:1613–  
694 1628.
- 695 Oba, G., E. Post, P. Syvertsen, and N. Stenseth. 2000. Bush cover and range condition  
696 assessments in relation to landscape and grazing in southern Ethiopia. *Landscape*  
697 *ecology* **15**:535–546.
- 698 Pan, S., and G. Lin. 2012. Invasion traveling wave solutions of a competitive system  
699 with dispersal. *Boundary Value Problems* **2012**:120.
- 700 Parizek, B., C. M. Rostagno, and R. Sottini. 2002. Soil erosion as affected by shrub  
701 encroachment in northeastern Patagonia. *Rangeland Ecology & Management/Journal*  
702 *of Range Management Archives* **55**:43–48.
- 703 Peters, D. P., and J. Yao. 2012. Long-term experimental loss of foundation species:  
704 consequences for dynamics at ecotones across heterogeneous landscapes. *Ecosphere*  
705 **3**:1–23.
- 706 Ratajczak, Z., J. B. Nippert, and S. L. Collins. 2012. Woody encroachment decreases  
707 diversity across North American grasslands and savannas. *Ecology* **93**:697–703.
- 708 Raupach, M. 1994. Simplified expressions for vegetation roughness length and zero-

709 plane displacement as functions of canopy height and area index. *Boundary-Layer*  
710 *Meteorology* **71**:211–216.

711 Ravi, S., P. D’Odorico, S. L. Collins, and T. E. Huxman. 2009. Can biological invasions  
712 induce desertification? *The New Phytologist* **181**:512–515.

713 Reed, M., L. Stringer, A. Dougill, J. Perkins, J. Athopheng, K. Mulale, and N. Favretto.  
714 2015. Reorienting land degradation towards sustainable land management: Linking  
715 sustainable livelihoods with ecosystem services in rangeland systems. *Journal of envi-*  
716 *ronmental management* **151**:472–485.

717 Reynolds, J. F., R. A. Virginia, P. R. Kemp, A. G. De Soyza, and D. C. Tremmel. 1999.  
718 Impact of drought on desert shrubs: effects of seasonality and degree of resource island  
719 development. *Ecological Monographs* **69**:69–106.

720 Roques, K., T. O’connor, and A. R. Watkinson. 2001. Dynamics of shrub encroach-  
721 ment in an African savanna: relative influences of fire, herbivory, rainfall and density  
722 dependence. *Journal of Applied Ecology* **38**:268–280.

723 Schlesinger, W. H., and A. M. Pilmanis. 1998. Plant-soil interactions in deserts. *Biogeo-*  
724 *chemistry* **42**:169–187.

725 Schlesinger, W. H., J. A. Raikes, A. E. Hartley, and A. F. Cross. 1996. On the spatial  
726 pattern of soil nutrients in desert ecosystems: ecological archives E077-002. *Ecology*  
727 **77**:364–374.

728 Schlesinger, W. H., J. F. Reynolds, G. L. Cunningham, L. F. Huenneke, W. M. Jarrell,  
729 R. A. Virginia, and W. G. Whitford. 1990. Biological feedbacks in global desertification.  
730 *Science* **247**:1043–1048.

731 Sirami, C., and A. Monadjem. 2012. Changes in bird communities in Swaziland savannas

732 between 1998 and 2008 owing to shrub encroachment. *Diversity and Distributions*  
733 **18**:390–400.

734 Skarpaas, O., and K. Shea. 2007. Dispersal patterns, dispersal mechanisms, and invasion  
735 wave speeds for invasive thistles. *The American Naturalist* **170**:421–430.

736 Sullivan, L. L., B. Li, T. E. Miller, M. G. Neubert, and A. K. Shaw. 2017. Density depen-  
737 dence in demography and dispersal generates fluctuating invasion speeds. *Proceedings*  
738 *of the National Academy of Sciences* **114**:5053–5058.

739 Taylor, C. M., and A. Hastings. 2005. Allee effects in biological invasions. *Ecology*  
740 *Letters* **8**:895–908.

741 Thompson, S. E., S. Assouline, L. Chen, A. Trahktenbrot, T. Svoray, and G. G. Katul.  
742 2014. Secondary dispersal driven by overland flow in drylands: Review and mechanistic  
743 model development. *Movement ecology* **2**:7.

744 Trollope, W., F. Hobson, J. Danckwerts, and J. Van Niekerk. 1989. Encroachment and  
745 control of undesirable plants. *Veld management in the Eastern Cape* pages 73–89.

746 Turnbull, L., J. Wainwright, and R. E. Brazier. 2010. Changes in hydrology and erosion  
747 over a transition from grassland to shrubland. *Hydrological Processes: An Interna-*  
748 *tional Journal* **24**:393–414.

749 Van Auken, O. 2009. Causes and consequences of woody plant encroachment into western  
750 North American grasslands. *Journal of environmental management* **90**:2931–2942.

751 Van Auken, O. W. 2000. Shrub invasions of North American semiarid grasslands. *Annual*  
752 *review of ecology and systematics* **31**:197–215.

753 Vasek, F. C. 1980. Creosote bush: Long-lived clones in the Mojave Desert. *American*  
754 *Journal of Botany* **67**:246–255.

- 755 Veit, R. R., and M. A. Lewis. 1996. Dispersal, population growth, and the Allee ef-  
756 fect: dynamics of the house finch invasion of eastern North America. *The American*  
757 *Naturalist* **148**:255–274.
- 758 Wang, M.-H., M. Kot, and M. G. Neubert. 2002. Integrodifference equations, Allee  
759 effects, and invasions. *Journal of mathematical biology* **44**:150–168.
- 760 Wells, P. V., and J. H. Hunziker. 1976. Origin of the creosote bush (*Larrea*) deserts of  
761 southwestern North America. *Annals of the Missouri Botanical Garden* pages 843–861.
- 762 Whitford, W., E. Depree, and P. Johnson. 1980. Foraging ecology of two chihuahuan  
763 desert ant species: *Novomessor cockerelli* and *Novomessor albigaster*. *Insectes Sociaux*  
764 **27**:148–156.
- 765 Whitford, W. G. 1978. Structure and seasonal activity of Chihuahua desert ant commu-  
766 nities. *Insectes Sociaux* **25**:79–88.
- 767 Wiernga, J. 1993. Representative roughness parameters for homogeneous terrain.  
768 *Boundary-Layer Meteorology* **63**:323–363.
- 769 Wood, S. 2017. *Generalized Additive Models: An Introduction with R*. 2 edition.  
770 Chapman and Hall/CRC.